Energy 150 (2018) 877–889

Contents lists available at ScienceDirect

Energy

journal homepage: www.elsevier.com/locate/energy

Adaptive model predictive control with propulsion load estimation and prediction for all-electric ship energy management

Jun Hou [a, *], Jing Sun [a, b], Heath Hofmann [a]

[a] Department of Electrical Engineering and Computer Science, University of Michigan, Ann Arbor, MI 48109, USA
[b] Department of Naval Architecture and Marine Engineering, University of Michigan, Ann Arbor, MI 48109, USA

ARTICLE INFO

Article history:
Received 23 June 2017
Received in revised form
25 January 2018
Accepted 3 March 2018
Available online 6 March 2018

Keywords:
Propulsion-load torque estimation and prediction
Adaptive model predictive control
All-electric ship
Hybrid energy storage
Energy management strategy

ABSTRACT

Electric ships experience large propulsion-load fluctuations on their drive shaft due to encountered waves and the rotational motion of the propeller, affecting the reliability of the shipboard power network and causing wear and tear. To address the load fluctuations, model predictive control has been explored as an effective solution. However, the load torque of the propulsion system, knowledge of which is essential for model predictive control, is difficult to measure and includes multi-frequency fluctuations. To deal with this issue, an adaptive model predictive control is developed so that the load torque estimation and prediction can be incorporated into model predictive control. In order to evaluate the effectiveness of the proposed adaptive model predictive control, an input observer with linear prediction is developed as an alternative approach to obtain the load estimation and prediction. Comparative studies are performed to illustrate the importance of the load torque estimation and prediction, and demonstrate the effectiveness of the proposed adaptive model predictive control in terms of improved efficiency, enhanced reliability and reduced wear and tear.

1. Introduction

Integrated power system (IPS), which is the key enabling technology of All-Electric Ship (AES) [1], provides the electrical power for both ship service and electric propulsion loads by integrating power generation, distribution, storage, and conversion [2]. Although IPS offers considerable benefits to modern ships, technical challenges exist in order to fully realize those benefits. For example, the propulsion load fluctuations experienced by the propeller, which also exist in traditional mechanical drive systems, have very different implication because of the inter-connectivity brought in by the IPS, as these fluctuations can affect the electrical shipboard network through the electric motors and their drives. This problem calls for new solutions that could effectively address the load fluctuations to assure reliability and integrity of the overall electrical network.

Three different propulsion load fluctuations have been studied in the literature:

- fluctuations resulting from the impact of the first-order wave at the encounter-wave frequency,
- fluctuations arising from the in-and-out-of-water effect,
- fluctuations caused by propeller rotation at the propeller-blade frequency (i.e., number of blades times shaft speed in rps).

These fluctuations, especially when the propeller is in-and-out-of-water, will cause unpredictable power consumption, reduce electrical efficiency, and affect power quality on the shipboard power network. The fluctuations caused by the in-and-out-of-water effect can be as high as 100% of the rated load. The load fluctuations caused by the encountered wave and the in-and-out-of-water effect are defined as low-frequency fluctuations in this paper. The fluctuations caused by the propeller rotation at the propeller-blade frequency are defined as high-frequency fluctuations. The impact of propeller-load fluctuations has been reported in the literature. In Ref. [3], the power combined with torque control was developed to deal with the low-frequency load fluctuations. The importance of torque balance is discussed in Ref. [4]. The torque unbalance is responsible for the propeller wear and tear. The in-an-out-of-water effect has been studied in Ref. [5]. These high-frequency fluctuations are reported as one of the main causes for severe mechanical wear and tear of the propulsion unit [5]. In

* Corresponding author.
E-mail addresses: junhou@umich.edu (J. Hou), jingsun@umich.edu (J. Sun), hofmann@umich.edu (H. Hofmann).

https://doi.org/10.1016/j.energy.2018.03.019
0360-5442/

Nomenclature

A_e/A_o	Expanded blade-area ratio
C_{UC}	Capacitance of ultra-capacitor
C_{Bus}	Capacitance of DC bus
D	Propeller diameter
G_{PG}	DC gain of generator set model
H	Total inertia
I_B, I_{UC}	Current of battery and ultra-capacitor
J_A, K_T, K_Q	Advance, thrust, and torque coefficients
N_B, N_{UC}, N_{Gen}	Number of battery modules, ultra-capacitor modules and generator sets
N	Predictive horizon
N_T	Performance investigation window
$n, Pitch/D$	Propeller rotational speed and pitch ratio
P_B, P_{UC}	Output power of battery and ultra-capacitor
P_{Gen}^{ref}, P_M^{ref}	Reference power of generator and motor
Q_B	Capacity of battery
R_n	Propeller Reynolds number
R_B, R_{UC}	Internal resistance of battery and ultra-capacitor
SOC_B, SOC_{UC}	SOC of battery and ultra-capacitor
T_{load}	Propeller-load torque
T_s	Sampling time
V_{max}	Maximum voltage of ultra-capacitor
V_{OC}	Battery open circuit voltage
V_d	Desired DC bus voltage
w	Wake field
Z	Number of propeller blades
β	Loss factor
β_M	Viscous damping coefficient of the motor and propeller
β_{LP}	Linear prediction coefficient
ρ	Water density
η_M	Efficiency of the motor and its inverter
λ	Weighting factor
ξ_L	Measurement noise
τ_{PG}	Time constant of generator set model
ω_d	desired motor rotational speed
AES	All-electric ship
AMPC	Adaptive model predictive control
EMS	Energy management strategy
HESS	Hybrid energy storage system
IO	Input observer
IPS	Integrated power system
LP	Linear prediction
PM	Prime mover
UC	Ultra-capacitor

Ref. [6], the high-frequency load fluctuations caused by wake field are studied. The experimental results of both low and high frequency fluctuations in Ref. [7] showed the significant negative effect of load fluctuations.

In order to address the impact of propulsion-load fluctuations, hybrid energy storage system (HESS) can be a potential solution. HESS has been exploited for considerable applications, such as hybrid electric vehicle [8], micro-grid [9] and all-electric ship [10], in order to provide complementary characteristics and achieve desired performance. In this paper, HESS serves as a buffer to absorb power when the propulsion motor is under-loaded and supply power when it is overloaded, thereby isolating the electric shipboard network from propulsion load fluctuations. The effectiveness of the proposal HESS solution highly depends on the system energy management strategy (EMS). In order to achieve robust and efficient operation and to meet various dynamic operational requirements, optimization-based EMS has been suggested in the Naval Power Systems Technology Development Roadmap [11]. More specifically, an effective EMS should provide improved fuel efficiency, enhanced response speed, superior reliability, and reduced mechanical wear and tear. Given the unique characteristics of IPS in AESs, as highlighted in Ref. [12] that include: nonlinear and multi-input-multi-output plant characteristics, multi-scale time dynamics, and multiple operating constraints, model predictive control (MPC) emerges as the natural choice for optimization-based EMS [13–15].

In Ref. [13], battery modules are controlled by MPC to assist the turbine and fuel cell in tracking the power command. In Ref. [14], the MPC is developed to reduce the pulse power effect. In order to reduce wear and tear on the generator sets, batteries are used in Ref. [15] to “smooth” the generator power by using MPC. The literature mentioned above do not require the propulsion-load torque information, since the control objectives and applications are different. In this manuscript, the propulsion-load torque is important to reduce the mechanical wear and tear and enhance the system reliability. In most marine applications, however, the propulsion-load torque is difficult to measure and includes multi-frequency fluctuations. Given the importance of the propulsion-load torque for the proposed EMS using MPC, this paper focuses on its estimation and prediction.

Load-torque estimation has been explored in a number of studies [16–18]. In Refs. [16,17], the load torque is assumed to be constant or slowly time-varying. The literature [16] focuses on the low-frequency load torque estimation, and the constant disturbance torque estimation is addressed in Ref. [17] for permanent magnet synchronous motor. For our problem, however, the load torque investigated here consists of multi-frequency fluctuation components. The input observer (IO) approach presented in Ref. [18], on the other hand, is not based on the assumption that the load torque is constant or slowly time-varying. Note that the input observer is also referred to as a disturbance observer in the literature, since an unknown input can be considered as a disturbance [19]. Despite the contributions of these works, the aforementioned approaches do not take advantage of the physical characteristics of the propulsion-load dynamics, especially the fast dynamics. Furthermore, these approaches cannot be directly used to predict the future load torque, which is required for implementing MPC. Additional load predictive capabilities are therefore required. In this paper, linear prediction (LP) is used to predict future load information. On the other hand, a model-based approach can be easily integrated with the MPC to formulate an Adaptive MPC (AMPC) to estimate and predict propulsion-load torque. However, the complexity of the propulsion-load model is the main challenge for real-time applications.

In this paper, a system-level energy management strategy is developed using model predictive control. The motivation of this paper is to mitigate the negative effect of both low and high frequency load fluctuations on the shipboard network. This proposed strategy encompasses the controls of the primary power sources and propulsion motor, in addition to the HESS, and allows judicious coordination to achieve desired performance in terms of increased system efficiency, enhanced reliability, reduced mechanical wear

and tear, and improved load-following capability. This paper focuses on the propulsion-torque estimation and prediction for implementing the proposed MPC-based EMS. The main contributions of this research are summarized in the following:

- An integrated EMS is developed to fully coordinate generator sets, HESS, and motor drive. The integrated approach takes advantage of the predictive nature of MPC and allows the designers to judiciously coordinate the different entities of the shipboard network under constraints, thereby providing benefits to system performance.
- The proposed MPC formulation is able to achieve comprehensive performance in terms of improved efficiency, enhanced reliability, and reduced mechanical wear and tear. Different control strategies, such as power, speed and torque control, are integrated into one MPC-based EMS.
- Two different approaches, namely adaptive model predictive control and input observer with linear prediction, are developed to estimate and predict propulsion-load torque. The effectiveness and limitations of these two approaches are evaluated.
- A simplified propulsion-load torque model is developed for the proposed adaptive MPC to reduce the computational complexity and facilitate the real-time capability.

The paper is organized as follows. In Section 2, the shipboard electrical propulsion system is described and the integrated EMS using MPC is presented. The proposed AMPC approach and the alternative approach (i.e., IO with LP) are developed in Section 3. The comparison study is performed in Section 4, and results are presented to illustrate the effectiveness of the proposed AMPC. Section 5 concludes this paper with a discussion of the results.

2. System description and adaptive model predictive control formulation

The schematic of the electric propulsion system under investigation is shown in Fig. 1. In this propulsion system, electric power is generated by prime mover and generator (PM/G) sets, and the propulsion thrust is generated by electric motor(s). The motor is mechanically connected with the propeller, so that the propulsion torque generated by the propeller becomes the load torque of the motor, as shown in Fig. 2 [10]. Due to the encountered waves and the rotational motion of the propeller, this propulsion-load torque contains multi-frequency fluctuations which affect the system reliability and efficiency. The HESS is used to isolate the power fluctuations from the DC bus in order to mitigate the effects of these fluctuations. The inverter and DC/DC converters are used to control the motor and HESS, respectively. Medium voltage DC (MVDC) power generation is used as the architecture of the shipboard network in this paper. MVDC is able to decouple prime mover speed from the frequency of the bus, leading to optimization of the generator for each type of prime mover without having to incorporate gears and without being restricted to rotational speed or a given number of poles. The benefits of MVDC include: reduced power conversion, increased power density, the elimination of transformers, and advanced reconfigurability [20].

In order to achieve complementary characteristics, two different HESS configurations, namely batteries with ultra-capacitors (UC) and batteries with flywheels, are taken into consideration. Batteries have high energy density, while UCs have high power density. Compared to batteries and UC, flywheels offer an intermediate choice with respect to energy and power density. Both of UC and flywheel have long cycle life, which can be used to extend the battery cycle life by a well-developed control strategy. As discussed in Ref. [21], the battery/flywheel configuration outperforms battery/ultra-capacitor at high sea states. At nominal or low sea states, such as sea states 4 and 2, the battery/ultra-capacitor has better performance than battery/flywheel. Note that, the proposed algorithm does not depend on the HESS configuration, so that both of those two configurations can be used in this paper. Because of the full coordination of the proposed AMPC, motor and generators can help HESS mitigate the negative effect of load fluctuations, especially at high sea states, where battery/flywheel configuration has better performance. Therefore, the battery/ultra-capacitor configuration is used in this paper.

2.1. Optimization-oriented dynamic model and operational constraints

The electric power generation system includes diesel-generator sets and their associated rectifiers. The diesel engine is used as the prime mover (PM), and is connected to the synchronous field-winding generator to provide AC power. The rectifier converts AC power into DC power. A speed regulator is used to control the diesel engine so as to keep the generator at the reference speed. In order to develop a control-oriented model, a linearized model of the electric power generation system is developed in this section. The field-winding voltage of the generator is defined as the control variable u_G, and the DC output current of the diode rectifier is defined as the state variable x_G. The DC bus voltage is assumed as the reference value when linearizing the power generation system. The dynamic models described in this paper are discretized using the Euler method with sampling time T_s. Therefore, the electric power generation system can be described as:

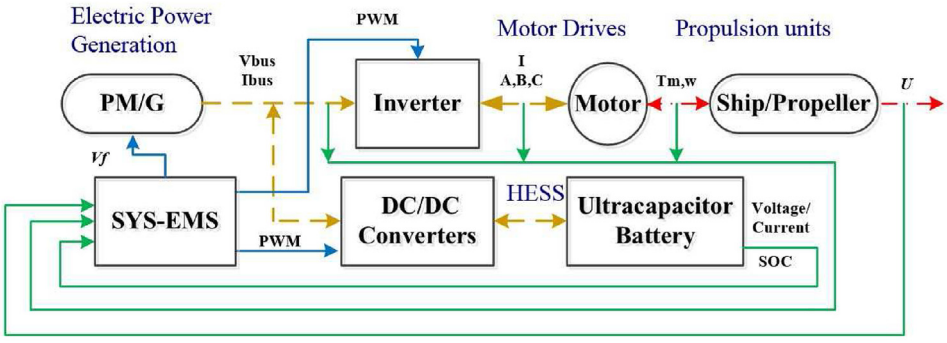

Fig. 1. Schematic of the electric propulsion system with HESS.

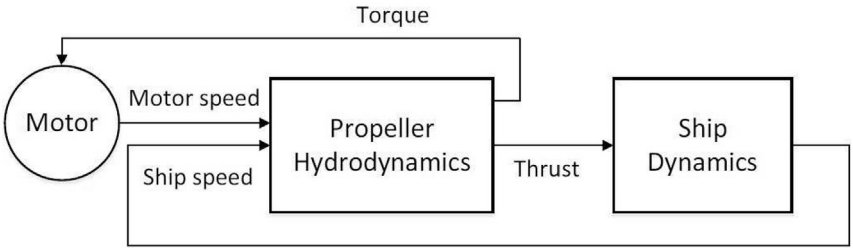

Fig. 2. Propeller and ship dynamics model structure [10].

$$x_G(k+1) = x_G(k) + \frac{T_s}{\tau_{PG}}(-x_G(k) + G_{PG}u_G(k)), \tag{1}$$

where τ_{PG} and G_{PG} are the time constant and DC gain of the linearized generator set model, respectively.

For the propulsion motor, the control variable u_M is the torque command, and the state variable x_M is the shaft rotational speed. The motor shaft dynamic system can be described in the following:

$$x_M(k+1) = x_M(k) + \frac{T_s}{H}(-\beta_M x_M(k) + u_M(k) - T_{Load}(k)), \tag{2}$$

where β_M is the viscous damping coefficient of the motor and propeller, H is the total inertia, and T_{Load} is the load torque.

The state of charge (SOC) of the battery pack and UC modules used in the HESS configurations are defined as the state variables x_B and x_{UC}, respectively, and the battery and UC currents as the control inputs u_B and u_{UC}, respectively. The HESS dynamic model is therefore described as follows:

$$\begin{aligned} x_B(k+1) &= x_B(k) - \frac{T_s}{3600Q_B}u_B(k), \\ x_{UC}(k+1) &= x_{UC}(k) - \frac{T_s}{V_{max}C_{UC}}u_{UC}(k), \end{aligned} \tag{3}$$

where Q_B is the capacity of the battery, and C_{UC} and V_{max} are the capacitance and the maximum voltage of the UC, respectively. Note that the HESS discharge is defined as the positive direction in this paper.

The total power output of battery and UC are obtained as follows:

$$\begin{aligned} P_B &= N_B \times \left(V_{OC}u_B - R_B u_B^2\right), \\ P_{UC} &= N_{UC} \times \left(V_{max}x_{UC}u_{UC} - R_{UC}u_{UC}^2\right), \end{aligned} \tag{4}$$

where N_B and N_{UC} are the number of modules, and R_B and R_{UC} are the internal resistance of the battery and UC modules, respectively.

The DC bus voltage dynamics are based on current flow into the bus capacitor, and the voltage of the DC bus is defined as the state variable x_{DC}. The DC bus dynamic model is expressed as follows:

$$\begin{aligned} x_{DC}(k+1) = x_{DC}(k) &+ \frac{T_s}{C_{Bus}x_{DC}(k)}(P_B(u_B(k)) + P_{UC}(x_{UC}(k), u_{UC}(k))) \\ &+ \frac{T_s}{C_{Bus}x_{DC}(k)}(N_{Gen}x_G(k)x_{DC}(k) - x_M(k)u_M(k)/\eta_M), \end{aligned} \tag{5}$$

where C_{Bus} is the DC bus capacitance, N_{Gen} is the number of generator sets, and η_M is the efficiency of the motor and its inverter.

The state variables and control inputs of the optimization-oriented model are summarized in Table 1. The system has several constraints, including state constraints and control input constraints, that represent hardware limitations and operational requirements. These constraints are mathematically expressed in the following:

Table 1
State variables and control inputs in the optimization-oriented design model.

Variable	Symbol	Description
State variables	x_G	Generator DC output current (A)
	x_M	Motor rotational speed (rad/s)
	x_B	Battery SOC (%)
	x_{UC}	Ultra-capacitor SOC (%)
	x_{DC}	DC bus voltage (V)
Control inputs	u_G	Generator field-winding voltage (V)
	u_M	Motor torque (Nm)
	u_B	Battery output current (A)
	u_{UC}	Ultra-capacitor output current (A)

$$\begin{aligned} &0 \le x_G \le 1000A, \\ &0 \le x_M \le 160RPM, \\ &20\% \le x_B \le 90\%, \\ &75\% \le x_{UC} \le 99\%, \\ &-10V \le u_G \le 10V, \\ &-1.25 \times 10^6 Nm \le u_M \le 1.25 \times 10^6 Nm \\ &-200A \le u_B \le 200A, \\ &-240A \le u_{UC} \le 240A. \end{aligned} \tag{6}$$

2.2. Control objectives

For the electric propulsion system, one of the main objectives is to generate the required thrust to move the ship forward at the desired speed. This is accomplished by controlling the motor speed, torque, or power to follow the references. Motor speed control is the most commonly used solution [5]. Besides thrust production, system reliability is also an important objective [14]. Due to the load fluctuations, especially when the propeller is in-and-out of water, the shipboard power network can experience large voltage variations which could significantly affect system operation. Therefore, voltage regulation is necessary. Other objectives, including system efficiency improvement and wear-and-tear reduction, are also taken into consideration. In order to improve system efficiency, the generator set and motor should operate at their most efficient operating points [14]. Furthermore, the HESS losses should be minimized. For the motor and propeller, the mechanical wear and tear is mainly caused by transients and oscillations in the shaft torque [5]. For the generator set, the mitigation of power oscillations can contribute to a reduction of mechanical wear and tear [15]. Since the DC bus voltage is close to its reference, the

Table 2
Control objectives, descriptions and their mathematical expression for the electric propulsion system with HESS.

Control objectives	Mathematical expression	Descriptions
System reliability	$\min(V_d - x_{DC}(k))^2$	Minimize bus voltage variation to maintain the system reliability.
Thrust production	$\min(\omega_d - x_M(k))^2$	Follow desired motor rotational speed to achieve the desired thrust.
System efficiency	$\min(P_{Gen}^{ref} - x_G(k)x_{DC}(k))^2$	Follow the reference to operate the generator at the high-efficiency point.
	$\min(P_M^{ref} - x_M(k)u_M(k))^2$	Follow the reference to operate the motor at the high-efficiency point.
	$\min(R_B u_B^2(k) + R_{UC}u_{UC}^2(k))$	Minimize HESS losses.
Wear-and-tear mitigation	$\min(x_G(k+1) - x_G(k))^2$	Minimize generator oscillations to reduce wear and tear on the generator set.
	$\min(u_M(k) - u_M(k-1))^2$	Minimize motor torque oscillations to reduce wear and tear on the motor and propeller.
	$\min(x_M(k+1) - x_M(k))^2$	Minimize speed oscillations to balance the motor torque and the load torque.

oscillation of the generator DC output current (i.e., x_G) is minimized in the optimization. The control objectives and their mathematical expression are summarized in Table 2, where V_d is the desired bus voltage, ω_d is the desired reference speed of the propulsion motor, and P_{Gen}^{ref} and P_M^{ref} are the reference powers of the generator sets and motor, respectively.

2.3. Adaptive model predictive control problem formulation

Given the nature of the electric propulsion system, as well as the operational constraints involved, MPC becomes a natural formulation. Since the propulsion-load torque T_{Load} in (2) is difficult to measure for marine applications, estimation of T_{Load} is required. Furthermore, in order to implement MPC, prediction of T_{Load} in the MPC prediction windows is also required. To address the estimation and prediction of the propulsion-load torque, an adaptive MPC is developed which minimizes a cost function subject to constraints within the prediction horizon. This can be mathematically expressed as follows:

$$P(x_0): \min_{x:[t,t+N]\to R^5 u:[t,t+N-1]\to R^4} J\left(x, u, \widehat{T}_{Load}\right) \tag{7}$$

where:

$$J\left(x, u, \widehat{T}_{Load}\right) = \Phi(x(t+N)) + \sum_{k=t}^{t+N-1} L\left(x(k), u(k), \widehat{T}_{Load}(k|t)\right), \tag{8}$$

subject to:

$$x(k+1) = f\left(x(k), u(k), \widehat{T}_{Load}(k|t)\right), x(t) = x_0, \tag{9}$$

$$C(x(k), u(k)) \le 0, \tag{10}$$

where $\Phi(x(N))$ and $L(x(k), u(k), \widehat{T}_{Load}(k|t))$ are the terminal and instantaneous cost functions, N is the time window over which the cost will be evaluated, $C(x(k), u(k))$ represents the inequality constraints, t represents the current time, and $x(k)$, $u(k)$ are the instantaneous values of the states and controls at time k, respectively. $\widehat{T}_{Load}(t|t)$ is the estimation of the propulsion-load torque, and $\widehat{T}_{Load}(k|t)$ for $k = t+1, \ldots, t+N-1$ are the predictions of the load torque at time t.

According to the aforementioned dynamic models and control objectives, the AMPC formulation takes the following form:

$$\Phi(x(N)) = \lambda_{VDC}(V_d - x_{DC}(N))^2 + \lambda_\omega(\omega_d - x_M(N))^2, \tag{11}$$

$$\begin{aligned} L\left(x(k), u(k), \widehat{T}_{Load}(k|t)\right) = {} & \lambda_{VDC}(V_d - x_{DC}(k))^2 \\ & + \lambda_\omega(\omega_d - x_M(k))^2 \\ & + \lambda_{P_{Gen}}\left(P_{Gen}^{ref} - x_G(k)x_{DC}(k)\right)^2 \\ & + \lambda_{P_M}\left(P_M^{ref} - x_M(k)u_M(k)\right)^2 \\ & + \lambda_{HESS}\left(R_B u_B^2(k) + R_{UC}u_{UC}^2(k)\right) \\ & + \lambda_{\Delta I_{PG}}(x_G(k+1) - x_G(k))^2 \\ & + \lambda_{\Delta T_M}(u_M(k) - u_M(k-1))^2 \\ & + \lambda_{\Delta\omega}(x_M(k+1) - x_M(k))^2, \end{aligned} \tag{12}$$

for all $k \in [t, t+N-1]$, subject to (1)–(3) and (5)–(6), where λ_{VDC}, λ_ω, $\lambda_{P_{Gen}}$, λ_{P_M}, λ_{HESS}, $\lambda_{\Delta I_{PG}}$, $\lambda_{\Delta T_M}$ and $\lambda_{\Delta\omega}$ are the weighting factors for the penalties of DC bus voltage variation, tracking performance of motor speed, generator and motor power, HESS losses, variations of generator output DC current, motor torque and motor speed, respectively. The estimation and prediction of propulsion load torque is addressed in the following section.

Remark 2.1. *(Motor control):* Motor speed control has the best performance on the thrust production, but can cause more mechanical wear and tear and introduce power fluctuations on the shipboard network. Motor power control can significantly mitigate power fluctuations on the shipboard network, but can cause significant mechanical wear and tear, especially when the propeller is in-and-out of water. Motor torque control can reduce the mechanical wear and tear if the propulsion-load torque is known, but has worse performance on thrust production and generate more power fluctuations. As shown in Equation (12), the proposed AMPC integrates all of these three control strategies: motor speed control term "$\lambda_\omega(\omega_d - x_M(k))^2$", motor power control term "$\lambda_{P_M}(P_M^{ref} - x_M(k)u_M(k))^2$" and motor torque control term "$\lambda_{\Delta T_M}(u_M(k) - u_M(k-1))^2$". Therefore, the comprehensive performance can be achieved.

Remark 2.2. *(Generator control):* Similar to motor control, the generator power control $\lambda_{P_{Gen}}(P_{Gen}^{ref} - x_G(k)x_{DC}(k))^2$ and bus voltage regulation $\lambda_{VDC}(V_d - x_{DC}(k))^2$ are integrated into AMPC. The benefits of power control and voltage regulation can be achieved.

Remark 2.3. *(Full-coordinated control):* The proposed AMPC also provide a full-coordinated control for the shipboard system. The motor, generators and HESS are all connected into the DC bus. The DC bus voltage can be used to identify the stability of DC ship power systems [22]. In order to maintain the bus voltage stable (minimizing $\lambda_{VDC}(V_d - x_{DC}(k))^2$), the motor and generators can assist HESS to mitigate load fluctuations, especially at high sea states

where the HESS cannot fully address the load fluctuations. Furthermore, undesirable interactions among motor, generators and HESS can be avoided.

3. Propulsion-load torque estimation and prediction

In order to take advantage of the physical characteristics of the propulsion-load dynamics, a model-based approach is developed to estimate the propulsion-load torque for all-electric ships. Due to the complexity of the propulsion-load torque model, a simplified model is developed first, which is able to capture the key dynamics. Because of uncertainties in the model parameters, adaptive parameter identification is used, leading to improved robustness of the control system. This model-based approach can be easily integrated with the MPC to formulate an AMPC. In order to evaluate the proposed AMPC approach, the IO presented in Ref. [18] is used as an alternative approach to estimate the propeller-load torque. In this alternative approach, linear prediction [23] is combined with IO to predict the future propulsion-load torque. A comparative study is performed to evaluate the effectiveness of the proposed AMPC, in terms of minimizing bus voltage variation, regulating rotational speed, and reducing high-frequency motor torque variation. The implications of accurate estimation and prediction are also illustrated and analyzed in this study.

3.1. First approach: input observer with linear prediction

In order to estimate the propulsion load torque, the input observer (IO) presented in Ref. [18] is used. The general propeller-motor dynamic is described by the following equation:

$$\dot{\omega} = \frac{T_M(t) - \beta_M \omega - T_{Load}(t)}{H}. \tag{13}$$

Define

$$\begin{aligned} u_L(t) &= T_{Load}(t)/H, \\ z_L(t) &= \frac{T_M(t) - \beta_M \omega(t)}{H}, \\ y_L(t) &= \omega(t) + \xi_L(t), \end{aligned} \tag{14}$$

where $\xi_L(t)$ is the measurement noise.

The unknown input $u_L(t)$ can be then estimated by the following equations [18]:

$$\begin{aligned} \hat{u}_L(t) &= \varepsilon_L(t) + \alpha_L y(t) + \phi_L(t), \\ \dot{\phi}_L &= -\alpha_L \phi_L - \alpha_L z_L, \\ \dot{\varepsilon}_L &= -\alpha_L \varepsilon_L - \alpha_L^2 y_L, \\ \hat{T}_{Load}(t) &= \hat{u}_L(t) H, \end{aligned} \tag{15}$$

where $\alpha_L > 0$ is the observer gain and the states of the observer are ϕ_L and ε_L.

Since the input observer cannot predict future load torque, linear prediction is used. Linear prediction incorporates the knowledge of the signal frequency spectrum and autocorrelation to determine the linear prediction coefficients (LPCs) [24]. Only past data, which can be obtained from IO estimation results, is required for LP. To predict the load torque at time t+1, linear prediction is formulated as follows:

$$\hat{T}_{Load}(t+1|t) = \sum_{i=1}^{N_{LP}} \beta_{LP_i} \hat{T}_{Load}(t-i+1|t), \tag{16}$$

where N_{LP} is the prediction order, and β_{LP_i} $(i = 1, \ldots, N_{LP})$ are the linear prediction coefficients. The coefficients can be calculated using the Matlab function "lpc". The inputs of "lpc" are the past data and the desired prediction order. The next step is to combine IO with LP. The algorithm can be easily implemented, as shown in Fig. 3. However, there are several limitations of this approach, summarized in the following:

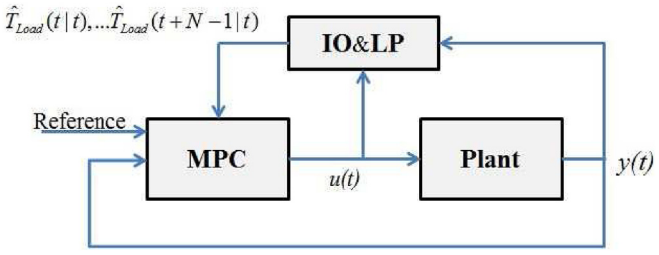

Fig. 3. Schematic diagram of the first approach (IO-LP).

Remark 3.1. The gain α_L in (15) is the only parameter used to tune IO. Since the high-frequency fluctuation is at the propeller-blade frequency, i.e., around 8Hz, the minimum cut-off frequency is designed at 8Hz, leading to a minimum observer gain $\alpha_L = 50$. As shown in Fig. 4, the phase shift at the cut-off frequency is about 45°, which could significantly affect the estimation performance. In order to reduce the estimation error, the high-gain input observer is a reasonable choice if the noise can be ignored. However, noise is an issue under many conditions; the estimation performance of a high-gain observer, e.g. $\alpha_L = 400$, might be even worse than one using the minimum gain. The optimum observer gain is difficult to determine when the noise is random and unknown.

Remark 3.2. The predictive performance of LP highly depends on past data. The performance of IO directly affects LP. Furthermore, the predictive error is accumulated as the predictive horizon extends. For example, predicting $\hat{T}_{Load}(t+2|t)$ requires the prediction value $\hat{T}_{Load}(t+1|t)$, which means the predictive error of $\hat{T}_{Load}(t+1|t)$ affects the prediction $\hat{T}_{Load}(t+2|t)$.

Since only the general propeller-motor model (13) is used in this approach, the dynamics of the propeller load torque is not taken

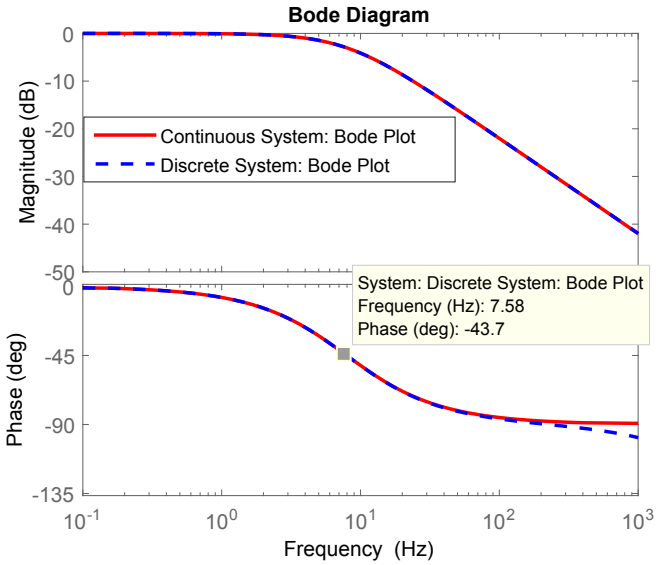

Fig. 4. Bode plot of the input observer.

into consideration. In order to address the limitations discussed in Remarks 3.1 and 3.2, a model-based approach is required, leading to the adaptive model predictive control discussed in the next section. The major challenge of this approach is the complexity of the load torque model (17). The focus of the next section is to develop a simplified model of (17), which is able to capture the key dynamics of the propeller-load torque.

3.2. Second approach: adaptive model predictive control

Instead of the general propeller-motor model (13), the propeller-load torque model presented in (17) can provide additional useful information to estimate the load torque. This propulsion-load torque model is expressed in the following:

$$\begin{aligned} T_{Load}(t) &= \mathrm{sgn}(n)\beta\rho n^2 D^5 f_{K_Q}(J_A, Pitch/D, A_e/A_o, Z, R_n) \\ &= \mathrm{sgn}(n)\beta\rho D^5\left(c_0 n^2 + c_1\frac{U(1-w)}{D}n\right) \\ &\quad +\mathrm{sgn}(n)\beta\rho D^5 c_2\left(\frac{U(1-w)}{D}\right)^2 \\ &\quad +\mathrm{sgn}(n)\beta\rho D^5\frac{c_3}{n}\left(\frac{U(1-w)}{D}\right)^3, \end{aligned} \tag{17}$$

where,

$$\begin{aligned} n &= \omega/2\pi, \\ 1-w &= M_0 - M_1 cos(4\theta), \end{aligned}$$

c_i (i = 0,1,2,3), M_0 and M_1 are unknown parameters; β is the loss factor; ρ is the density of water; D is the diameter of the propeller; f_{K_Q} is the torque coefficient function; and θ is the angular position of one blade (this angular position is assumed to be measurable). In f_{K_Q}, J_A is the advance coefficient; $Pitch/D$ is the pitch ratio; A_e/A_o is the expanded blade-area ratio, with A_e being the expanded blade area and A_o being the swept area; Z is the number of propeller blades; and R_n is the Reynolds number.

The parameters in (17) are usually fitted off-line. For example, parameters $c_{0,1,2,3}$ in the function f_{K_Q} are based on the fitted K_Q curves for the Wageningen B-Series Propellers [25] and the K_Q correction multiplier [26]. The multiplier in Ref. [26] is chosen to minimize the error in the range of maximum efficiency. If the propeller is not operating in the maximum efficiency range, the error could be enlarged significantly. Furthermore, the coefficients in f_{K_Q} can vary with the wear and tear of the propeller. As the operating environment changes, the parameters in the propeller-load model (17) can also change. Therefore, to use (17) for load torque estimation, online parameter identification is necessary.

In this detailed load model (17), six parameters $c_0, c_1, c_2, c_3, M_0, M_1$ are used in the nonlinear parametric model, making parameter estimation difficult. To facilitate online parameter estimation, the following simplified model (18) is proposed, whose derivation is given in the Appendix.

$$T_{Load} \approx \overline{C}_1 + \overline{C}_2 cos(4\theta) + \overline{C}_3\left(n - n_{ref}\right). \tag{18}$$

The output of the detailed propeller-load torque model and the simplified model (18) at sea state 4 and 6 are shown in Fig. 5.

With the combination of (13) and (18), the new propeller-motor model is developed in the following:

$$\dot{\omega} = \frac{T_M(t) - \beta_M\omega - \left(\overline{C}_1 + \overline{C}_2 cos(4\theta) + \overline{C}_3\Delta\omega/2\pi\right)}{H}. \tag{19}$$

For parameter estimation, the parametric model is defined in the following:

$$z_{par} = C_{par}^{*T}\phi_{par}, \tag{20}$$

where,

$$\begin{aligned} z_{par} &= \left\{\frac{\lambda_{par}}{s+\lambda_{par}}\right\}\left(\dot{\omega} - \frac{1}{H}(T_M - \beta_M\omega)\right), \\ C_{par}^{*} &= \left[\overline{C}_1 \;\; \overline{C}_2 \;\; \overline{C}_3\right]^T, \\ \phi_{par} &= \left\{\frac{-\lambda_{par}}{s+\lambda_{par}}\right\}[1 \;\; cos(4\theta) \;\; \Delta\omega/2\pi]^T, \end{aligned}$$

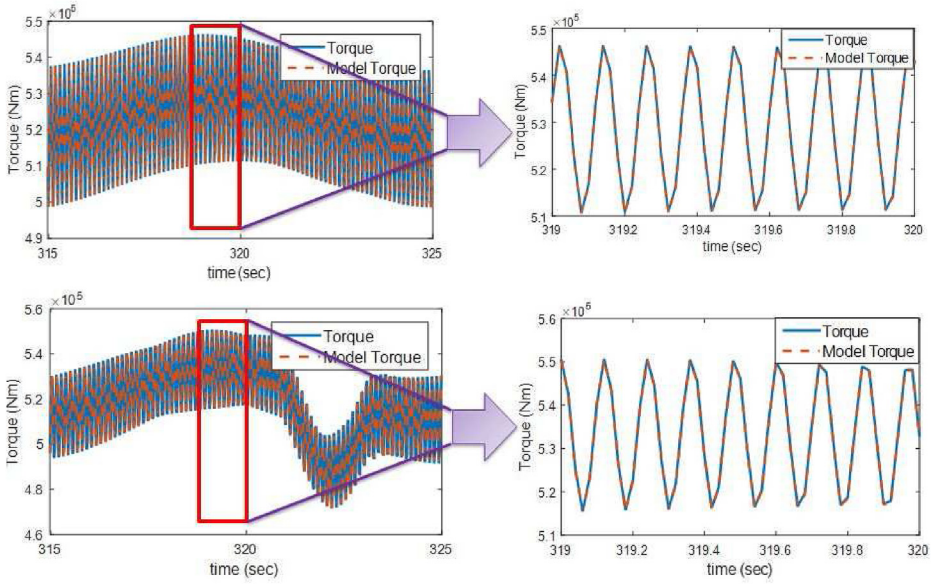

Fig. 5. Outputs of the detailed and simplified propeller-load torque models at sea state 4 (top) and sea state 6 (bottom).

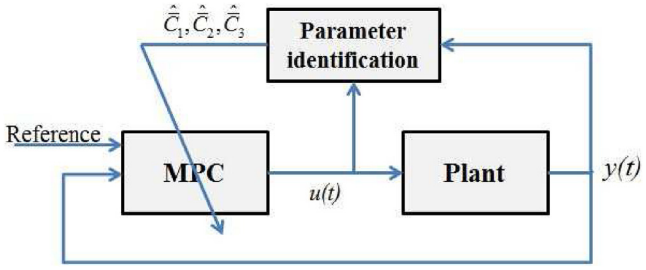

Fig. 6. Schematic diagram of the AMPC controller.

λ_{par} is the filter gain, and $\{\cdot\}$ represents the dynamic operator of the filter, whose transfer function is $(\cdot)$. The filter is introduced to avoid taking numerical derivatives in estimation.

The normalized gradient algorithm is chosen as the adaptive law, and presented in the following [27]:

$$C_{par}(k) = C_{par}(k-1) + \frac{T_s \Gamma \phi_{par}(k) \varepsilon_{par}}{1 + \phi_{par}(k)^T \phi_{par}(k)},$$

where

$$\varepsilon_{par} = z_{par}(k) - C_{par}(k-1)^T \phi_{par}(k),$$

and $\Gamma = \Gamma^T$ is a positive-definite matrix, satisfying the real part of the eigen-values of Γ is between $(0, 2/T_s)$, which affects how fast C_{par} updates.

The speed variation within the predictive horizon is assumed to be very small, i.e., $x_M(t+N-1) \approx x_M(t+N-2) \approx \ldots \approx x_M(t)$. This results in an estimation of the future propeller-blade position at time k as follows:

$$\theta(k) = \theta(t) + (k-t) T_s x_M(t). \quad (t \le k \le t+N-1)$$

Therefore, the schematic diagram of the proposed AMPC is shown in Fig. 6, and the new propeller-motor dynamic is expressed in the following:

$$\begin{aligned} x_M(k+1) &= x_M(k) - \frac{T_s \overline{C}_3}{2\pi H}(x_M(k) - \omega_d) \\ &+ \frac{T_s}{H}\left(u_M(k) - \beta_M x_M(k) - \overline{C}_1\right) \\ &- \frac{T_s}{H}\overline{C}_2 cos(4(\theta(t) + (k-t) T_s x_M(t))). \end{aligned} \quad (21)$$

Table 3
Ship parameters [21].

Description	Parameter	Value
Ship length	L_{ship}	190 m
Ship breadth	B_{ship}	28.4 m
Draft	H	15.8 m
Mass	m	20000 ton
Added-mass	m_x	28755 ton
Thrust deduction coefficient	t_d	0.2
Propeller diameter	D	5.6 m
Wetted area	S	12297 m^2
Advance facing area in the air	A_T	675.2 m^2
Water resistance coefficients	$C_F + C_R$	0.0043
Air resistance coefficient	C_{air}	0.8

Table 4
Parameters for simulation in two sea states [21].

Description	Parameter	Value
Wave period	T_{wave}	12 sec
Wave height	h_{wave}	2m (SS4)/4m (SS6)
Wave length	L_{wave}	40.29%L_{ship}
Ship speed command	U_d	12.4 knot

4. Performance evaluation and discussion

To quantitatively compare and analyze the performance of the proposed algorithm, two sea states (SS4 and SS6), corresponding to moderate and severe operating conditions, respectively, are used in the performance evaluation. Ship parameters as well as waves information are shown in Tables 3 and 4 [21]. Because the negative effects of load fluctuations at high sea states are much more significant than those at low sea states and HESS can fully address the load fluctuations at low sea states (such as sea state 2), the low sea states (such as sea state 2) are not reported in this paper.

According to the control objectives, the performance metrics are presented in Table 5, where N_T equals $[(t_T - t_0)/T_s]$, with $[\cdot]$ being the integer rounding of, and t_0 and t_T are the initial and final values of the time period being investigated. In this paper, the sampling time T_s is 0.02 s and the investigation time is 60 s (about 5 wave periods). In order to evaluate the proposed approaches to load torque estimation and prediction, results obtained from six cases have been studied and analyzed in this section. These six cases are described in the following:

- Case 1, "Ideal": In this case, the actual propulsion-load torque (17), without any uncertainty, is used. Nonlinear MPC uses perfect knowledge to predict the future load torque in its optimization. Because there is no uncertainty in this case, it is referred to as "Ideal".
- Case 2, "Frozen prediction": In this case, the current load torque is obtained from the load torque model (17) without any uncertainty. Compared to Case 1, the future load torque used in the MPC is assumed to be same as the current load torque, i.e., $T_{Load}(t+N-1|t) = T_{Load}(t+N-2|t) = \ldots = T_{Load}(t|t)$.
- Case 3, "LP-Only": Different from Case 2, the future load torque in this case is predicted using linear prediction. The true value is used for the current load torque.

Table 5
Performance metrics.

Performance	Mathematical expression
Voltage Regulation	$\sqrt{\frac{\sum_{k=0}^{N_T}(V_d - x_{DC}(k))^2}{N_T+1}}$
Speed Regulation	$\sqrt{\frac{\sum_{k=0}^{N_T}(\omega_d - x_M(k))^2}{N_T+1}}$
Gen Power Tracking	$\sqrt{\frac{\sum_{k=0}^{N_T}(P_{Gen}^{ref} - x_{DC}(k)x_G(k))^2}{N_T+1}}$
Motor Power Tracking	$\sqrt{\frac{\sum_{k=0}^{N_T}(P_M^{ref} - x_M(k)u_M(k))^2}{N_T+1}}$
HESS Losses Reduction	$\sqrt{\frac{\sum_{k=0}^{N_T}(R_B u_B^2(k) + R_{UC} u_{UC}^2(k))}{N_T+1}}$
Gen Oscillation Reduction	$\sqrt{\frac{\sum_{k=0}^{N_T}(x_G(k+1) - x_G(k))^2}{N_T+1}}$
Torque Oscillation Reduction	$\sqrt{\frac{\sum_{k=0}^{N_T}(u_M(k) - u_M(k-1))^2}{N_T+1}}$
Speed Oscillation Reduction	$\sqrt{\frac{\sum_{k=0}^{N_T}(x_M(k+1) - x_M(k))^2}{N_T+1}}$
Total Cost	$\sqrt{\frac{\sum_{k=0}^{N_T} L(x(k), u(k), T_{Load}(k))}{N_T+1}}$

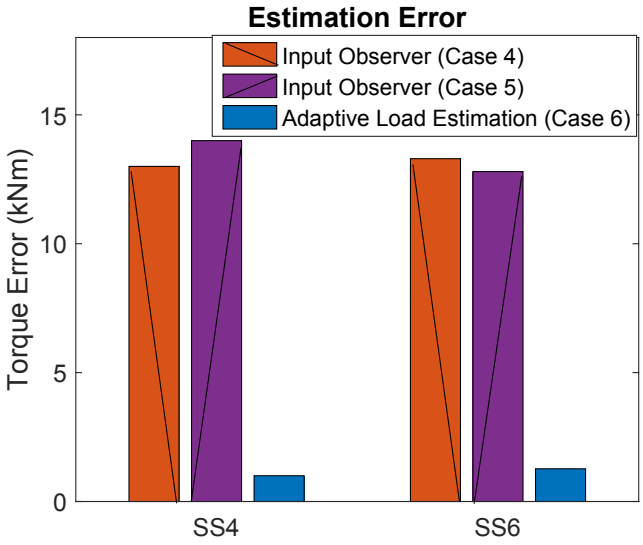

Fig. 7. Estimation error of the adaptive parameter identification and input observer.

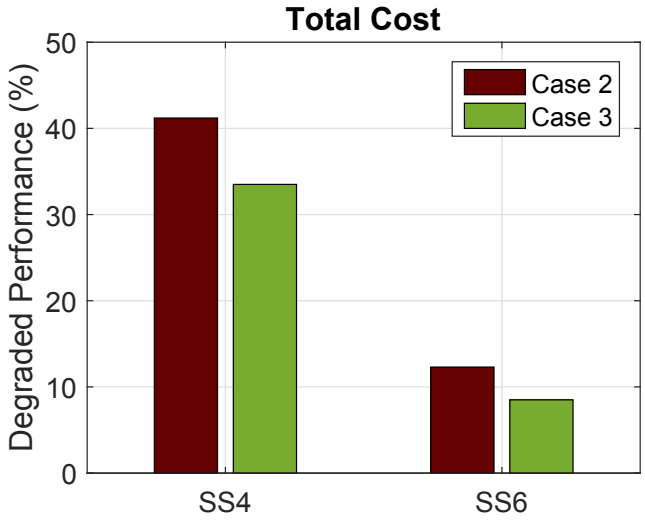

Fig. 8. Cases 2 and 3 degraded "Total Cost" performance compared to Case 1.

- Case 4, "IO-Only": In this case, the input observer is used, instead of the true load torque. The future load torque is assumed to be the same as the current IO estimation.
- Case 5, "IO-LP": The first approach, i.e., IO combined with LP, is used in this case.
- Case 6, "AMPC": This case is the proposed AMPC.

The estimation performance is evaluate first. Among these six cases, Cases 4, 5, and 6 require estimation of the load torque. As shown in Fig. 7, adaptive parameter identification has better estimation performance than the input observer. The reason is that more propeller-load information is taken into consideration in this adaptive approach.

The key performance metrics and results are presented in Table 6. The performance results of each case are normalized by Case 1. Smaller values represent better performance. Note that the performance of Cases 2–6 from best to worst are colored in the following sequence: **blue**, **green**, **yellow**, **brown** and **red**.

As can be seen in Table 6, the performance of Case 6 ("AMPC") is the closest to Case 1 ("Ideal"). Case 1 ("Ideal") uses the accurate detailed propeller-load model and takes its dynamics into consideration, leading to the best performance among all of the investigated cases. The "Total Cost" in the performance metrics represents the overall performance, which takes all of the other metrics along with their priorities (i.e., their weighting factors) into consideration. The mathematical expression of "total cost" is shown in Table 5. According to "Total Cost", the performance from the best to the worst are Case 1 ("Ideal"), Case 6 ("AMPC"), Case 3 ("LP-Only"), Case 2 ("Frozen prediction"), Case 5 ("IO-LP"), and Case 4 ("IO-Only") at both sea states 4 and 6. Based on the performance comparison, key observations are presented in the following *remarks*.

Remark 4.1. *(Effects of load prediction):* Cases 1 ("Ideal"), 2 ("Frozen prediction") and 3 ("LP-Only") all assume perfect load estimation at time t, but use different load predictions. Case 1 ("Ideal") takes the load dynamics into consideration, and Case 3 ("LP-Only") uses the signal spectrum and correlation information to

Table 6
Performance comparison.

Sea State 4.

Performance Metrics	Case 1	Case 2	Case 3	Case 4	Case 5	Case 6
"Voltage Regulation"	1	27.77	27.76	28.15	28.07	1.036
"Speed Regulation"	1	1.043	1.043	1.057	1.057	0.995
"Gen Power Tracking"	1	1.095	1.057	1.251	1.179	1.148
"Motor Power Tracking"	1	1.116	1.162	1.154	1.185	1.151
"HESS Losses Reduction"	1	1.185	1.189	1.247	1.227	1.184
"Gen Oscillation Reduction"	1	1.055	1.011	1.384	1.286	0.985
"Torque Oscillation Reduction"	1	2.803	1.792	3.067	2.609	2.172
"Speed Oscillation Reduction"	1	1.186	1.178	1.198	1.194	1.025
"Total Cost"	**1**	1.412	1.335	1.456	1.414	1.106

Sea State 6.

"Bus Regulation"	1	24.63	24.61	24.97	24.97	1.328
"Speed Regulation"	1	1.032	1.029	1.045	1.045	1.027
"Gen Power Tracking"	1	1.267	1.254	1.438	1.318	1.241
"Motor Power Tracking"	1	1.147	1.144	1.163	1.151	1.099
"HESS Losses Reduction"	1	1.166	1.174	1.189	1.197	1.194
"Gen Oscillation Reduction"	1	1.307	1.578	2.167	1.649	1.128
"Torque Oscillation Reduction"	1	2.206	1.590	2.376	2.178	1.230
"Speed Oscillation Reduction"	1	1.216	1.196	1.246	1.242	1.052
"Total Cost"	**1**	1.123	1.085	1.149	1.130	1.009

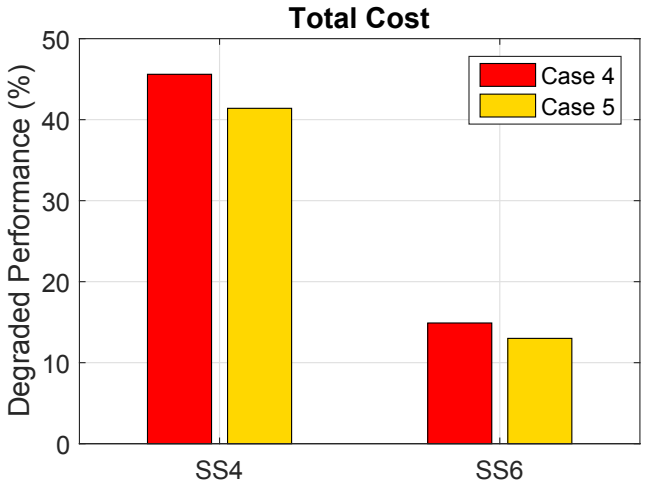

Fig. 9. Cases 4 and 5 degraded "Total Cost" performance compared to Case 1.

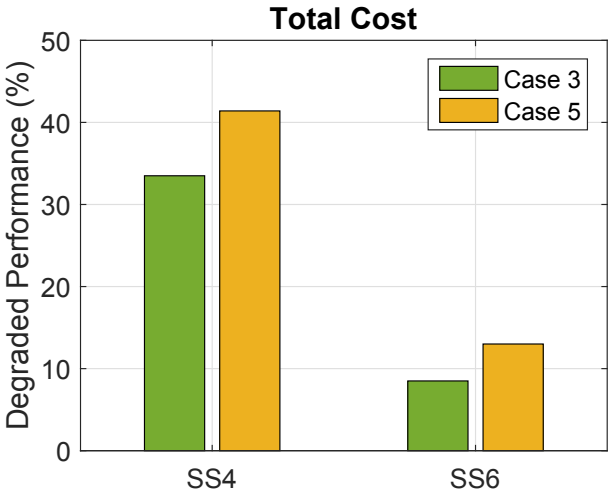

Fig. 11. Cases 3 and 5 degraded "Total Cost" performance compared to Case 1.

predict future torque, while Case 2 ("Frozen prediction") uses none of these, leading to the worst performance of the three cases. The "Total Cost" performance degradation of Cases 2 ("Frozen prediction") and 3 ("LP-Only") compared to Case 1 ("Ideal") is shown in Fig. 8. Because all the performance values of Case 1 ("Ideal") are one, performance degradation (%) can be expressed that the performance values of Case 2–5 minus one and then time 100%. Another comparative result can be shown between Cases 4 ("IO-Only") and 5 ("IO-LP"). Both Cases 4 ("IO-Only") and 5 ("IO-LP") use the input observer to estimate $\widehat{T}_{load}(t|t)$, but differ in the prediction scheme. The "Total Cost" degradation of Cases 4 ("IO-Only") and 5 ("IO-LP") compared to Case 1 ("Ideal") is shown Fig. 9. Note that the difference between Cases 4 ("IO-Only") and 5 ("IO-LP") is smaller than that between Cases 2 ("Frozen prediction") and 3 ("LP-Only"), because the estimation error in Case 5 ("IO-LP") influences the prediction performance.

Remark 4.2. *(Effects of load estimation):* The difference between Case 2 ("Frozen prediction") and Case 4 ("IO-Only") is in the load torque estimation, where the former uses the actual load torque but the latter employs an IO to estimate the load torque. Case 2 ("Frozen prediction") outperforms Case 4 ("IO-Only") in terms of most of the performance metrics. Their "Total Cost" performance is shown in Fig. 10. Similarly, Case 3 ("LP-Only") and Case 5 ("IO-LP") use the same prediction method, but have different load estimation. As shown in Fig. 11, the difference between Cases 3 ("LP-Only") and 5 ("IO-LP") is larger than that between Cases 2 ("Frozen prediction") and 4 ("IO-Only"). This is because the estimation affects not only the instantaneous information, but also the prediction in Cases 3 ("LP-Only") and 5 ("IO-LP"). Case 1 ("Ideal") has better performance than Case 6 ("AMPC") as expected, due to the uncertainties in the dynamic model used for Case 6 ("AMPC"). These comparisons demonstrate that load torque estimation plays a key role in achieving good performance.

Remark 4.3. *(Effects of data-based LP):* Except for Cases 1 ("Ideal") and 6 ("AMPC"), Case 3 ("LP-Only") has the best performance among the remaining 4 cases. Even though Case 3 ("LP-Only") only uses a data-based load predictor, the prediction still contributes some benefits, especially with regard to reducing wear and tear. As shown in Fig. 12, metric "Torque Oscillation Reduction" demonstrates that Case 3 ("LP-Only") can achieve almost the same small motor torque variations as Case 6 ("AMPC"). Moreover, Case 3 ("LP-Only") outperforms Cases 2 ("Frozen prediction"), 4 ("IO-Only") and 5 ("IO-LP") in terms of metrics "Gen Oscillation Reduction" and "Speed Oscillation Reduction", as shown in Table 6, further

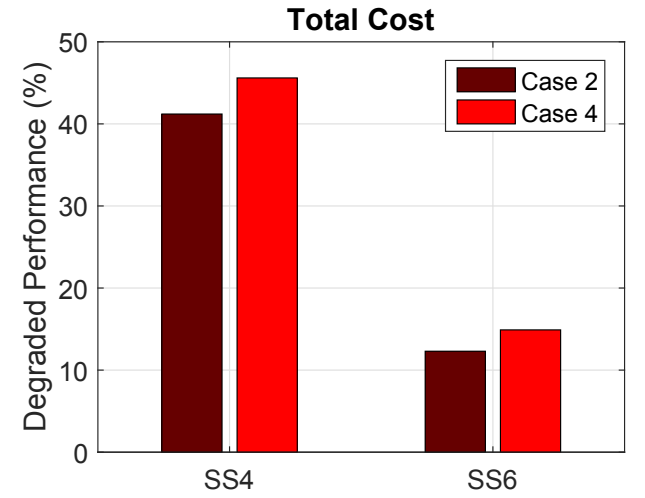

Fig. 10. Cases 2 and 4 degraded "Total Cost" performance compared to Case 1.

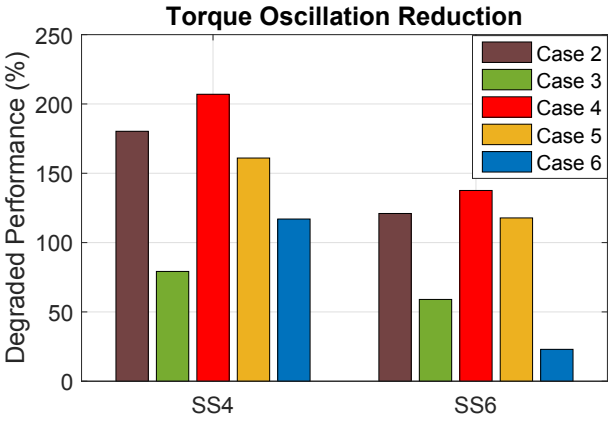

Fig. 12. Cases 2–6 degraded "Torque Oscillation Reduction" performance compared to Case 1.

Table 7
Performance comparison: Case 6 vs. Case 1 with 2% modeling error.

Performance Metrics	SS4		SS6	
	Case 6	2%Err	Case 6	2%Err
"Voltage Regulation"	1.036	11.26	1.328	9.125
"Speed Regulation"	0.995	2.074	1.027	1.585
"Gen Power Tracking"	1.148	3.226	1.241	1.827
"Motor Power Tracking"	1.151	1.598	1.099	7.829
"HESS Losses Reduction"	1.184	3.438	1.194	1.502
"Gen Oscillation Reduction"	0.985	4.038	1.128	2.885
"Torque Oscillation Reduction"	2.172	1.467	1.230	1.155
"Speed Oscillation Reduction"	1.006	1.014	1.052	1.02
"Total Cost"	1.106	2.190	1.009	1.410

demonstrating the benefits of LP in performance metrics of reducing the wear and tear of the motor and generator sets. Compared to Case 3 ("LP-Only"), Case 5 ("IO-LP") also uses LP to predict future torque. However, the estimation error of the input observer affects the prediction performance, as discussed in *Remark 4.2*. As can be seen, only at sea state 4 can Case 5 ("IO-LP") achieve performance similar to Case 2 ("Frozen prediction"). At sea state 6, the performance of Case 5 ("IO-LP") is worse than Case 2 ("Frozen prediction"). This comparison illustrates that the load torque estimation is essential for improving the performance of data-based LP.

Remark 4.4. *(Effects of adaptation):* Case 6 ("AMPC") is the only case that achieves competitive performance to Case 1 ("Ideal"). This is because only in these two cases the load dynamics are truly captured by using the propulsion-load torque model, thereby maintaining the motor and generator sets working around the reference points through subsystem coordination. Without the ability to capture the load torque dynamics, however, other cases need the assistance of the motor and generator sets to mitigate the bus voltage variations, leading to degraded system efficiency and increased wear and tear. In order to evaluate the effects of adaptation, a comparative study is performed between Case 6 ("AMPC") and Case 1 ("Ideal") with 2% modeling errors (2%Err are added on c_0 and M_0). As shown in Table 7, most performance indices are very sensitive to modeling error. These 2% modeling errors (without adaptation) can cause "Total Cost" 100% and 40% higher than Case 6 (with adaptation) at sea state 4 and 6, respectively. Moreover, the performance is even much worse than Case 4 ("IO-Only"). The key factors that renders favorable performance of AMPC are summarized in the following:

- The foundation of AMPC is a well-developed simplified model that captures the essential dynamics of the load torque. With accurate parameter identification, AMPC can predict the future load torque much better than LP.
- When the load torque dynamic model is integrated into the MPC controller, AMPC truly takes the load torque dynamic into consideration, resulting in the unique advantage of AMPC compared to the other 4 cases (Case 2 ("Frozen prediction"), 3 ("LP-Only"), 4 ("IO-Only") and 5 ("IO-LP")).

Remark 4.5. *(Effects of weighting factors):* The weighting factors can undoubtedly influence the performance of the proposed AMPC. In this paper, each weighting factor λ assigns a relative priority to a performance attribute. Given the main objectives, the system reliability and thrust production have the highest priority. The weighting factor can be tuned to reflect different design emphasis. One performance metric can be improved by tuning its weighting factor, but this could result in other metrics being negatively

Table 8
Performance comparison: weighting factor effects.

Performance Metrics	Case 6	*Test 1*	*Test 2*
Sea State 4.			
"Voltage Regulation"	1.036	1.040	7.882
"Speed Regulation"	0.995	1.210	1.168
"Gen Power Tracking"	1.148	1.064	6.634
"Motor Power Tracking"	1.151	1.0185	0.697
"HESS Losses Reduction"	1.184	1.023	0.553
"Gen Oscillation Reduction"	0.985	1.075	7.522
"Torque Oscillation Reduction"	2.172	0.271	3.928
"Speed Oscillation Reduction"	1.025	1.006	1.065
Sea State 6.			
"Bus Regulation"	1.328	1.395	6.689
"Speed Regulation"	1.027	1.461	1.275
"Gen Power Tracking"	1.241	1.150	3.941
"Motor Power Tracking"	1.099	0.980	0.449
"HESS Losses Reduction"	1.194	1.017	0.390
"Gen Oscillation Reduction"	1.128	1.188	1.541
"Torque Oscillation Reduction"	1.230	0.418	1.314
"Speed Oscillation Reduction"	1.052	1.140	1.034

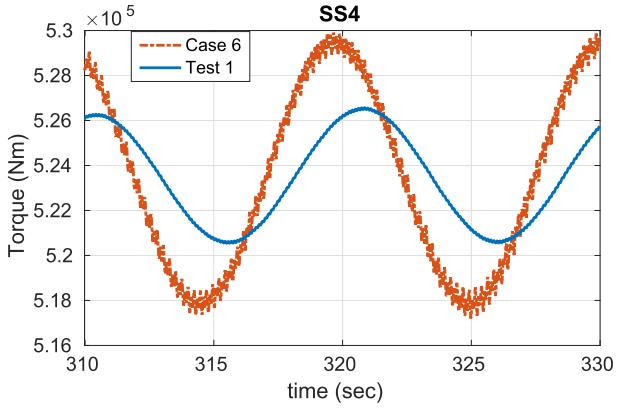

Fig. 13. Torque comparison (sea state 4): Case 6 vs. Test 1.

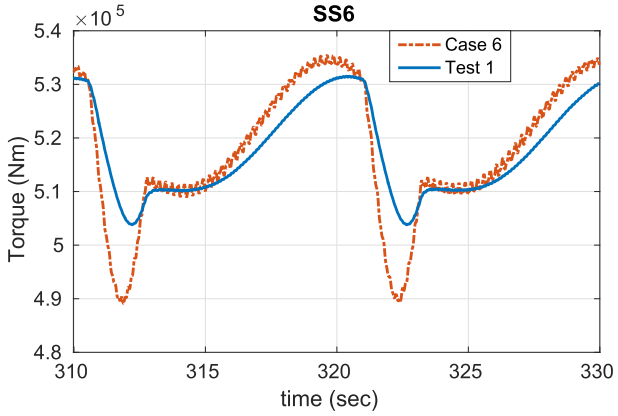

Fig. 14. Torque comparison (sea state 6): Case 6 vs. Test 1.

affected. Two tests are studied to demonstrate how the weighting factors affect the performance. These two tests are described in the following:

- *Test 1*: $10\lambda_{\Delta T_M}$ is used in this test to further reduce the motor torque oscillations.
- *Test 2*: $10\lambda_{HESS}$ is used with an emphasis on improving the energy efficiency of HESS.

As shown in Table 8, the motor torque oscillation has been significantly reduced by increasing the weighting factor $\lambda_{\Delta T_M}$ in Test 1 ($10\lambda_{\Delta T_M}$). As shown in Figs. 13 and 14, there is almost no motor torque oscillation in Test 1 ($10\lambda_{\Delta T_M}$). Similarly, the losses of HESS are significantly reduced in Test 2 ($10\lambda_{HESS}$). However, the high weighting factor λ_{HESS} forces the HESS to limit its operation at very low currents, leading to the loss of ability in isolating the load fluctuations from the DC bus. This causes negative effects on most of other performance metrics. Test 2 ($10\lambda_{HESS}$) also provides the insights into the importance of HESS in mitigating the effect of the load fluctuations.

5. Conclusion

This paper proposes a new energy management strategy, AMPC, to integrate power generation, electric motor, and hybrid energy storage control for electric ship propulsion systems in order to address the effects of propulsion-load fluctuations in the shipboard network. This approach addresses the estimation and prediction of the propulsion load torque. In order to evaluate the proposed AMPC, an alternative control is developed by integrating the input observer with linear prediction into the MPC strategy. Compared to the alternative approach, the proposed AMPC achieves much better performance in terms of improved system efficiency, enhanced reliability, improved thrust production, and reduced mechanical wear and tear. In addition to the alternative control, other cases are studied in this paper to illustrate the importance of the load estimation and prediction. In future work, computationally-efficient optimization algorithms for implementing the proposed EMS will be investigated.

Acknowledgment

This work was sponsored by the U.S. Office of Naval Research (ONR) under Grants No. 00014-15-1-2668. The authors would like to thank the editor and reviewers for their valuable feedback.

Appendix

Considering the propeller load torque model of (17) with $\bar{c}_i = \mathrm{sgn}(n)\beta\rho D^5 c_i \left(\frac{U}{D}\right)^i, (i = 0, 1, 2, 3)$ and $1 - w = M_0 - M_1 cos(4\theta)$, The derivation of the simplified model (18) is presented in the following:

$$
\begin{aligned}
T_{Load} &= \bar{c}_0 n^2 + \bar{c}_1(1-w)n + \bar{c}_2(1-w)^2 + \bar{c}_3(1-w)^3\frac{1}{n} \\
&= \bar{c}_0 n^2 + \bar{c}_1 M_0 n + \bar{c}_2\left(M_0^2 + 0.5M_1^2\right) + \frac{\bar{c}_3}{n}\left(M_0^3 + 1.5M_0M_1^2\right) \\
&\quad -\left(\bar{c}_1 M_1 n + 2\bar{c}_2 M_0 M_1 + 3\frac{\bar{c}_3}{n}M_1 M_0^2\right)cos(4\theta) \\
&\quad +\left(0.5\bar{c}_2 M_1^2 + 1.5\frac{\bar{c}_3}{n}M_0 M_1^2\right)cos(8\theta) - \bar{c}_3 M_1^3 cos(4\theta)^3 \\
&\approx \bar{c}_0 n^2 + \bar{c}_1 M_0 n + \bar{c}_2\left(M_0^2 + 0.5M_1^2\right) + \frac{\bar{c}_3}{n}\left(M_0^3 + 1.5M_0M_1^2\right) \\
&\quad -\left(\bar{c}_1 M_1 n + 2\bar{c}_2 M_0 M_1 + 3\bar{c}_3 M_1 M_0^2\frac{1}{n}\right)cos(4\theta) \\
&\approx \bar{c}_0\left(n_{ref}^2 + 2n_{ref}\Delta n\right) + \bar{c}_1 M_0\left(n_{ref} + \Delta n\right) \\
&\quad +\bar{c}_2\left(M_0^2 + 0.5M_1^2\right) + \bar{c}_3\frac{1}{n_{ref}}\left(M_0^3 + 1.5M_0M_1^2\right) \\
&\quad -\left(\bar{c}_1 M_1\left(n_{ref} + \Delta n\right) + 2\bar{c}_2 M_0 M_1 + 3\bar{c}_3 M_1 M_0^2\frac{1}{n_{ref}}\right)cos(4\theta) \\
&= \overline{C}_1 + \overline{C}_2 cos(4\theta) + \overline{C}_3\Delta n + \overline{C}_4\Delta n cos(4\theta) \\
&\approx \overline{C}_1 + \overline{C}_2 cos(4\theta) + \overline{C}_3\Delta n.
\end{aligned}
$$

where,

$$
\overline{C}_1 = \bar{c}_0 n_{ref}^2 + \bar{c}_1 M_0 n_{ref} + \bar{c}_2\left(M_0^2 + 0.5M_1^2\right) + \bar{c}_3\frac{1}{n_{ref}}\left(M_0^3 + 1.5M_0M_1^2\right),
$$

$$
\overline{C}_2 = -\left(\bar{c}_1 M_1 n_{ref} + 2\bar{c}_2 M_0 M_1 + 3\bar{c}_3 M_1 M_0^2\frac{1}{n_{ref}}\right),
$$

$$
\overline{C}_3 = 2n_{ref}\bar{c}_0 + \bar{c}_1 M_0,
$$

$$
\overline{C}_4 = -\bar{c}_1 M_1,
$$

$$
\Delta n = n - n_{ref}.
$$

The first step of simplification is to ignore the high-frequency

terms, i.e., $\left(0.5\bar{c}_2M_1^2+1.5\bar{c}_3M_0M_1^2\frac{1}{n}\right)cos(8\theta)-\bar{c}_3M_1^3cos(4\theta)^3$, which are greater than the propeller blade frequency. This is because the amplitudes of these high-frequency terms are much smaller than other terms, and they can be filtered significantly by the inertia of the propeller. The second step is to linearize the load torque model around the reference speed.

In this linearized model, the component $\overline{C}_4\Delta ncos(4\theta)$ only contains the variation terms, such as M_1, Δn, $cos(4\theta)$, and can be considered as a high order component. Because $\overline{C}_4\Delta ncos(4\theta)$ is much smaller than the other components, it can also be ignored. Finally, the linearized model $\overline{C}_1+\overline{C}_2cos(4\theta)+\overline{C}_3\Delta n$ has only three unknown parameters. According to the time-scale separation approach, these three parameters are assumed to be slowly time-varying.

References

[1] McCoy TJ. Electric ships past, present, and future [technology leaders]. IEEE Electr Mag 2015;3(2):4–11.
[2] Doerry N. Naval power systems: integrated power systems for the continuity of the electrical power supply. IEEE Electr Mag 2015;3(2):12–21.
[3] Sørensen AJ, Smogeli ØN. Torque and power control of electrically driven marine propellers. Control Eng Pract 2009;17(9):1053–64.
[4] Radan D. Integrated control of marine electrical power systems. Ph.D. dissertation. Norwegian University of Science and Technology; 2008.
[5] Smogeli ØN, Sørensen AJ. Antispin thruster control for ships. IEEE Trans Control Syst Technol 2009;17(6):1362–75.
[6] McCarthy J. On the calculation of thrust and torque fluctuations of propellers in non-uniform wake flow. Research and Development Report. Hydromechanics Laboratory; October 1961.
[7] Koushan K. Dynamics of propeller blade and duct loading on ventilated thrusters in dynamic positioning mode. In: DP conference, Houston; 2007. p. 1–13. October 9-10.
[8] Song Z, et al. Sliding-mode and Lyapunov function-based control for battery/supercapacitor hybrid energy storage system used in electric vehicles. Energy 2017;122:601–12.
[9] Sarrias-Mena R, et al. Fuzzy logic based power management strategy of a multi-MW doubly-fed induction generator wind turbine with battery and ultracapacitor. Energy 2014;70:561–76.
[10] Hou J, Sun J, Hofmann HF. Mitigating power fluctuations in electric ship propulsion with hybrid energy storage system: design and analysis. IEEE J Ocean Eng 2017;43(1).
[11] Kuseian J. Naval power systems technology development roadmap, Electric Ships Office. PMS 2013;320.
[12] Sun J. Optimisation-based control for electrified vehicles: challenges and opportunities. J Control Decis 2015;2(1):46–63.
[13] Seenumani G, Sun J, Peng H. Real-time power management of integrated power systems in all electric ships leveraging multi time scale property. IEEE Trans Control Syst Technol 2012;20(1):232–40.
[14] Park H, et al. Real-time model predictive control for shipboard power management using the ipa-sqp approach. IEEE Trans Control Syst Technol 2015;23(6):2129–43.
[15] Bø TI, Johansen TA. Battery power smoothing control in a marine electric power plant using nonlinear model predictive control. IEEE Trans Control Syst Technol 2016;25(4).
[16] Smogeli ØN. Control of marine propellers: from normal to extreme conditions. Ph.D. dissertation. Norwegian University of Science and Technology; 2006.
[17] Solsona J, Valla MI, Muravchik C. Nonlinear control of a permanent magnet synchronous motor with disturbance torque estimation. IEEE Trans Energy Convers 2000;15(2):163–8.
[18] Kolmanovsky I, Sivergina I, Sun J. Simultaneous input and parameter estimation with input observers and set-membership parameter bounding: theory and an automotive application. Int J Adapt Control Signal Process 2006;20(5):225–46.
[19] Chen W-H, Yang J, Guo L, Li S. Disturbance-observer-based control and related methods - an overview. IEEE Trans Ind Electron 2016;63(2):1083–95.
[20] Doerry N. Naval power system technology development Roadmap. Electric Ships Office, SEA 05; 2007.
[21] Hou J, Sun J, Hofmann H. Battery/flywheel hybrid energy storage to mitigate load fluctuations in electric ship propulsion systems. In: American control conference; 2017. p. 1296–301.
[22] Cupelli M, et al. Power flow control and network stability in an all-electric ship. Proc IEEE 2015;103(12):2355–80.
[23] Vaidyanathan P. The theory of linear prediction. Synth Lect Signal Process 2007;2(1):1–184.
[24] So HC, Chan KW, Chan YT, Ho KC. Linear prediction approach for efficient frequency estimation of multiple real sinusoids: algorithms and analyses. IEEE Trans Signal Process 2005;53(7):2290–305.
[25] Barnitsas M, Ray D, Kinley P. Kt, kq and efficiency curves for the wageningen b-series propellers. 1981.
[26] HydroComp. Kt, kq and efficiency curves for the wageningen b-series propellers. 2003.
[27] Ioannou PA, Sun J. Robust adaptive control. 2012.